



 Cite this: *RSC Adv.*, 2023, **13**, 34637

# Preparation and characterization of water-reducible polyester resin based on waste PET for insulation varnish

 Yong-A. Choe, Ri-Bom Pak, Su-Il Kim and Kyong-Sik Ju \*

Water-reducible polyester resin (WRPE) for insulation varnish was prepared from waste polyethylene terephthalate (PET), glycerol (GL), and phthalic anhydride (PA) *via* depolymerization and condensation. PET was depolymerized *via* glycolysis at different molar ratios of PET/GL (PET repeating unit/GL molar ratios: 1.6, 1.3, and 1.0) with zinc acetate as a catalyst at 220–230 °C. The resulting glycolytic products (GPs) were reacted with PA at contents of 5, 7.5, 10, 12.5, and 15 wt%, based on the total weight. The prepared WRPEs were dissolved in phenol, neutralized with aqueous ammonia to pH = 7–7.5, and diluted in water. The WRPEs were cured with hexamethoxymethyl melamine resin (HMMM, WRPE : HMMM = 70 : 30, based on the dry mass) at 140 °C for 2 h. The formation of GPs, WRPE, and WRPE-HMMM was investigated using Fourier transformer infrared spectroscopy and proton nuclear magnetic resonance spectroscopy; the thermal properties were characterized using thermogravimetric analysis and differential scanning calorimetry. The electrical insulation strength and volume resistivity of the cured films with PA content were investigated. This strength and volume resistivity first increased with increasing PA content and then decreased above 10 wt%. The results show that WRPE with a PA content of 10 wt% exhibits optimal insulation properties.

 Received 19th September 2023  
 Accepted 27th October 2023

DOI: 10.1039/d3ra06369k

[rsc.li/rsc-advances](https://rsc.li/rsc-advances)

## 1. Introduction

In the electrical industry, flexible polyester resin is essential for insulating materials to absorb heat shocks from the heating and cooling cycles of electrical coils.<sup>1,2</sup> Polyester insulation varnishes based on organic solvents usually contain of volatile organic compounds (VOCs) of 50–70%, which cause environmental deterioration. To address this challenge, studies have explored using water-borne and powder insulation coatings to reduce the use of VOCs.<sup>3,4</sup> Water-reducible varnish, among the water-borne coatings, contains copolymers formed *via* polymerization reactions that occur in water-miscible solvents such as alcohols or esters. Polar groups, such as the carboxyl group (–COOH) and sulfonic acid group (–SO<sub>3</sub>H), of the polymer allow water reducibility. Previously, a water-soluble polyester for insulation varnish was synthesized using thermal and catalytic condensation polymerization techniques.<sup>3</sup> However, monomers, such as trimellitic anhydride, terephthalic acid, diethylene glycol, and ethylene glycol, used in that study are petro-based raw materials produced *via* condensation polymerization. Currently, polyethylene terephthalate (PET) is widely used in packaging applications and other related fields due to its cost-effective production and good mechanical properties.<sup>5</sup> However, the poor biodegradability and large amount of PET waste have caused serious environmental problems. Therefore, various kinds of coatings, such as

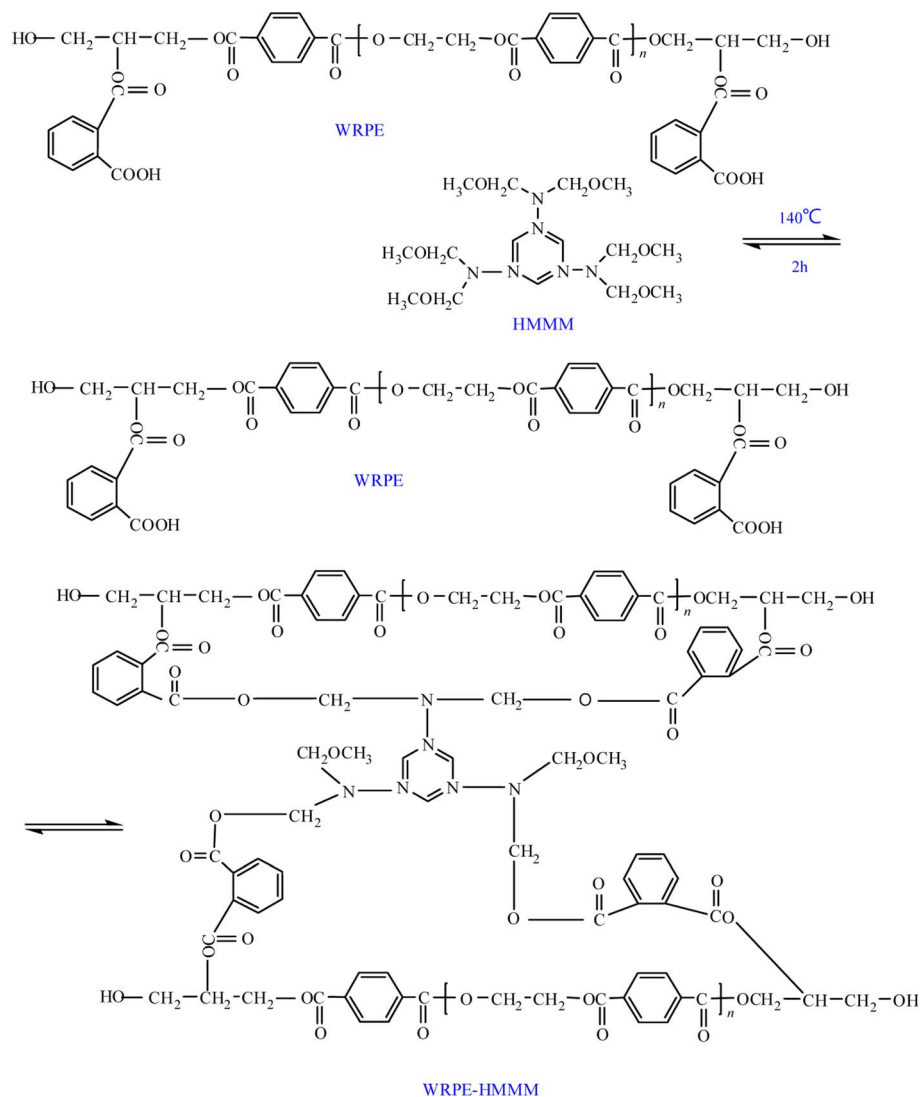
polyester,<sup>6–8</sup> alkyd,<sup>9–14</sup> unsaturated polyester,<sup>15–17</sup> and epoxy,<sup>18–20</sup> based on waste PET have been widely studied and used. Nonetheless, the preparation of water-reducible polyester insulation varnish using waste PET has not been reported. To prepare water-reducible polyester insulation varnish, chemical degradation of waste PET should be studied. Chemical degradation is common for PET recycling as it degrades the PET chain *via* chain scission using water, methanol, glycols, and polyamines in hydrolysis, alcoholysis, glycolysis, and aminolysis processes, respectively, with catalysts like zinc acetate.<sup>21,22</sup> The procedure for preparing water-reducible polyester resin (WRPE) involves incorporating polyvalent carboxylic groups into the main chain as hydrophilic groups, and this is to limit the molecular weight to a certain extent.<sup>23</sup> The most studied chemical recycling method involves a reaction between PET and various diols: ethylene glycol (EG), propylene glycol (PG), diethylene glycol (DEG), and dipropylene glycol (DPG).<sup>10,16,24</sup> However, glycolytic products (GPs) obtained through these methods have no reactive groups in the main chain. Glycerol (GL) is a triol and thus can react through its three hydroxyl groups; this structure has reactive groups. When PET is depolymerized by GL, the semicrystalline structure of PET may transform to an amorphous structure. Although GL is not a glycol, we presume that it reacts mainly over the two primary hydroxyls and thus for simplification we use the term “glycolysis”.<sup>25</sup>

Conversely, because GPs obtained *via* depolymerization of PET have relatively fewer hydrophilic groups, it is not water reducible. Phthalic anhydride (PA), containing one aromatic

High-Tech Research and Development Center, Kim Il Sung University, Pyongyang, Democratic People's Republic of Korea. E-mail: ks.ju1025@ryongnamsan.edu.kp







Scheme 3 Curing reaction of WRPE with HMMM.

to 160 °C for 0.5 h, and the reaction was performed at the same temperature for 1 h; AV of the product was measured. Then, the temperature was decreased to 100 °C, and the product was dissolved in phenol to produce an 80% (w/w) solution for 0.5 h. Subsequently, 25% aqueous ammonia was slowly added and the solution was neutralized to slightly alkaline (pH 7.5–8.0) at 40–50 °C; the product was filtered through a filter press.

#### 2.4. Curing of WRPE with HMMM

The prepared WRPE was blended with HMMM (weight ratio of 70 : 30 based on the dry mass), and the WRPE-HMMM mixture was diluted with water to adjust the viscosity. Then, varnishes on copper sheet were prepared by the immersion method and cured in an oven at 140 °C for 2 h.

#### 2.5. Characterization

Analysis of AV was conducted according to ASTM D 1639, *i.e.*, 1 ± 0.002 g of sample was dissolved in ethanol-toluene (1 : 1)

solution and titrated with 0.1 N KOH solution using phenolphthalein as a color indicator. HV was determined *via* a conventional acetic anhydride/pyridine method according to ASTM D 4276, and the viscosity was evaluated according to ASTM D 1545. The pH values were measured using a digital pH meter. The cured films were characterized *via* adhesion (ASTM D 3359), conical mandrel flexibility (ASTM D 522), impact strength (ASTM D 2794), and water resistance (ASTM D 1647). The chemical structures of GPs, WRPE, and WRPE-HMMM were characterized *via* Fourier transformer infrared spectroscopy (FTIR) and proton nuclear magnetic resonance spectroscopy (<sup>1</sup>H NMR). FTIR spectra were recorded with a Nicolet 6700 FTIR spectra-photometer (USA) in transmission mode, scanning from 4000 to 400 cm<sup>-1</sup>. <sup>1</sup>H NMR spectra (400 MHz, CDCl<sub>3</sub>) of the samples were recorded on a Bruker Avance 400 MHz spectrometer (Germany). Thermogravimetric analysis (TGA) of the dried films was conducted on a PerkinElmer TGA 4000 thermogravimetric analyzer (USA) under air atmospheres. Thermal analysis was conducted in the temperature range of



40–700 °C with a 20 °C min<sup>-1</sup> heating rate. Differential scanning calorimetry (DSC) was performed by a Mettler Toledo DSC-851e (Switzerland) under a nitrogen atmosphere at a flow of 20 mL min<sup>-1</sup>.

**2.5.1. Water-dispersible stability.** A  $\phi$  15 mm test tube was charged with WRPE solution (nonvolatile matter 40 wt%) to a 10 cm height, and the stability of the WRPE solution was evaluated at the time when the height of the separated water layer reached 1 cm.

**2.5.2. Electrical insulation properties.** The electrical insulation strength and volume resistivity were measured with a BERTAN tester (USA) and high resistivity meter (China). The varnishes on the copper sheet were prepared by the immersion method and cured in an oven at 140 °C for 2 h. The size of the copper sheet used as a substrate was 6.0 × 15.0 × 0.1 cm. Five measurements of the thickness for the cured films were measured and recorded as average values. The voltage was increased until electric breakdown at 25 ± 2 °C. The electrical insulation strength ( $E$ ) was determined as follows:

$$E = \frac{V}{d}$$

where the  $V$  is the breakdown voltage and  $d$  is the average thickness of the film (mm).

The volume resistivity ( $\rho_v$ ) was calculated as follows:

$$\rho_v = R_v \frac{A}{d}$$

where  $R_v$  is the volume resistance ( $\Omega$ ) and  $A$  is the area of the sample contacting the electrode (cm<sup>2</sup>).

## 3. Results and discussion

### 3.1. Glycolysis of PET with GL

In a previous study, glycols such as EG, DEG, and PG were often used for glycolysis of PET. The aim of this study is to use recycled GPs from waste PET as a potential raw material to prepare WRPE as an insulation varnish. To fulfill this goal, waste PET was depolymerized by GL. Generally, the preparation of water-reducible polymers involves incorporating carboxylic groups as hydrophilic groups in the main chain. GL has three hydroxyl groups—two primary and one secondary—and is easily obtained from biofuel production and agroindustrial waste. When GL reacts with GP, two unreacted hydroxyl groups (one primary and one secondary) remain in the GP from waste PET. The unreacted secondary hydroxyl group may be reacted with another monomer or oligomer, and hence, the semicrystalline structure of PET may transform to an amorphous or lower semicrystalline structure. In

addition, when PA is added, unreacted hydroxyl groups may react with PA to yield hydrophilic groups in the main chain. The glycolysis of PET by GL is the transesterification reaction of EG and GL. Given that the boiling point of EG is 197 °C, it is separated in the glycolysis of PET under vacuum pressure. The boiling point of GL is 290 °C, and it may easily react in the glycolysis of PET, instead of EG. Herein, the transesterification reaction was performed at different molar ratios of PET/GL (PET repeating unit/GL molar ratios of 1.6, 1.3, and 1.0) at 220–230 °C and 600–350 mmHg for 2.5 h (GP1–GP3). The HV, AV, and free EG amount separated from PET in the glycolysis of PET are provided in Table 1, which show that these values increased when the PET/GL molar ratio decreased from 1.3 to 1.0. This is due to the rapid glycolysis of PET upon increasing the GL amount. Subsequently, the molecular weight of the GP decreased with decreasing PET/GL molar ratio.

### 3.2. Esterification reaction

In a previous study, unsaturated polyester resin was prepared by reacting the GPs with maleic anhydride and PA at 170 °C.<sup>16</sup> To avoid linear or network condensation polymerization by PA and limit the average molecular weight of the prepared polyester resin, the reaction temperature must be lower than 170 °C. The water-dispersible stability generally increased upon increasing the carboxyl group content in the polymer chain and decreasing the average molecular weight of the polymer. GPs reacted with PA at contents of 5, 7.5, 10, 12.5, and 15 wt%, based on the total weight, at 160 °C for 1 h. The AV, viscosity, and water-dispersible stability of the WRPEs with different PET/GL molar ratios and PA contents are shown in Table 2. Here, the viscosity was measured in nonvolatile matter at 40 ± 2 wt%. As shown in Table 2, AV increased and viscosity decreased with decreasing PET/GL molar ratio from 1.6 to 1.0 at the same PA content. Further, the lower the PET/GL molar ratio, the better the water-dispersible stability of the WRPE. Conversely, AV and viscosity increased with increasing PA content at the same PET/GL molar ratio. In addition, it was observed that the higher the PA content, the better the water-dispersible stability of the WRPE. This is because the water-dispersible stability of WRPE essentially depends on the average molecular weight of GP and hydrophilic group content.

The average molecular weight of GP was determined in accordance with the PET/GL molar ratio, and the hydrophilic group content was related to PA content.

### 3.3. Dissolution and curing of WRPEs

WRPE varnish comprises a saturated polyester resin, high flash point nonreactive organic solvents as cosolvents, and water as

Table 1 Amount of HV, AV, and free EG separated from PET

Sample	Molar ratio of PET/GL	PET (g)	GL (g)	HV (mg KOH g <sup>-1</sup> )	AV (mg KOH g <sup>-1</sup> )	Free EG (g)
GP1	1.6	96	28.2	164.3	10.3	8.1
GP2	1.3	96	36.8	200.3	17.6	13.5
GP3	1.0	96	46	243.5	23.5	16.3



a diluent. Phenol, having high flash point ( $T_b = 182\text{ }^\circ\text{C}$ ) and good solubility, is a nonreactive organic solvent. Moreover, phenol is a polar solvent and may be mixed with water. WRPE varnish is prepared at approximately 40 wt% solid content and 60 wt% volatile solvent content (40 wt% of phenol and 60 wt% of deionized water, based on the total solvent weight). WRPE containing appreciable amounts of hydroxyl and carboxyl groups is rarely used as insulation varnish due to the poor water resistance of the films. HMMM, as a fully methylolated aminoplastic, is reactive with hydroxyl and carboxyl groups and miscible with water. HMMM also exhibits a tendency for crosslinking rather than self-condensation reaction, offering more functional sites for crosslinking, high reactivity with hydroxyl, carboxyl, or amine groups of the main polymer, and the potential for high crosslink density and water-dispersible stability.<sup>26</sup> Therefore, using HMMM as a curing agent can lower the curing temperature achieving satisfactory physico-chemical and insulation properties for the insulation varnish.

### 3.4. Chemical characterization of WRPEs

The results of the FTIR analysis for PET, GP, WRPE, and cured WRPE-HMMM are shown in Fig. 1. The FTIR spectra of PET and GP show that there are no changes to the skeleton structure as no observable changes are found. After the transesterification reaction, the absorption at  $2963\text{ cm}^{-1}$  decreased and that at  $3426\text{ cm}^{-1}$  increased, which is the result of the reaction of the hydroxyl groups produced by exchanged GL. From the FTIR spectra of GP and WRPE, C=O stretching vibration absorption at  $1720\text{ cm}^{-1}$ , C–O–C deformation vibration absorptions at  $1264$  and  $1121\text{ cm}^{-1}$ , OH absorption at  $3426\text{ cm}^{-1}$ , CH<sub>2</sub> signal vibration absorption at  $2963\text{ cm}^{-1}$ , in-plane deformation vibration of the benzene ring at  $1598\text{ cm}^{-1}$ , and C–H pendular oscillation absorption at  $729\text{ cm}^{-1}$  are observed. Further, the C=O signal vibration absorption at  $1721\text{ cm}^{-1}$  and C–O–C deformation vibration absorptions at  $1267$  and  $1104\text{ cm}^{-1}$  are shifted a little and more intense compared to GP, such that the esterification reaction by PA can be confirmed. Conversely, the

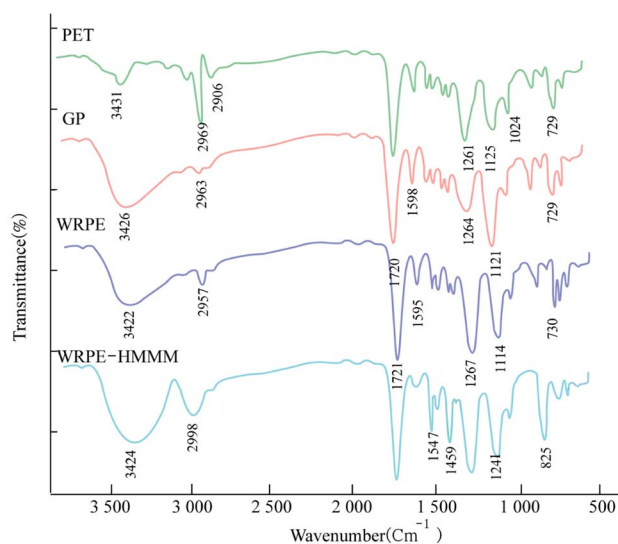


Fig. 1 FTIR spectra of PET, GP, WRPE, and WRPE-HMMM.

OH signal vibration absorption at  $3422\text{ cm}^{-1}$  is shifted more than before the reaction. Hence, it can be seen that the esterification reaction by the hydroxyl groups in the chain hardly occurs. In the FTIR spectrum of the WRPE-HMMM, the triazine ring out-of-plane deformation vibration at  $825\text{ cm}^{-1}$ , O=C=O linkages revealing strong absorption at  $1241\text{ cm}^{-1}$ , N–C–N bending and ring deformation at  $1547\text{ cm}^{-1}$ , and the free methyl group of HMMM being stable at  $1459\text{ cm}^{-1}$  are observed.

To further identify the structures, the <sup>1</sup>H NMR spectra of GP, WRPE, and WRPE-HMMM are shown in Fig. 2. In the GP spectrum, 3.75–3.82 ppm (peak *b*) indicates protons of methyl groups closer to the primary hydroxyl group, and 4.12–4.30 ppm (peak *d*) is related to the protons of the secondary primary hydroxyl group of GL. 4.50–4.62 ppm (peak *e*) indicates protons of methyl groups closer to the ester. 4.62–4.92 ppm (peak *a*) and 7.91–8.19 ppm (peak *f*) indicate protons of primary hydroxyl

Table 2 AV, viscosity, and water-dispersible stability of WRPEs with different PET/GL molar ratios and PA contents

Sample	Molar ratio of PET/GL	PA content (%)	AV (mg KOH g <sup>-1</sup> )	Viscosity (mpa s)	Water-dispersible stability (d)
WRPE11	1.6	5	25.9	448	—
WRPE12		7.5	32.8	473	—
WRPE13		10	44.2	507	—
WRPE14		12.5	49.3	539	3
WRPE15		15	64.6	580	10
WRPE21	1.3	5	28.4	393	10
WRPE22		7.5	35.4	420	25
WRPE23		10	46.2	454	Over 30
WRPE24		12.5	53.6	488	Over 30
WRPE25		15	69.6	524	Over 30
WRPE31	1.0	5	32.4	349	30
WRPE32		7.5	39.1	366	Over 30
WRPE33		10	53.5	403	Over 30
WRPE34		12.5	59.2	432	Over 30
WRPE35		15	74.2	459	Over 30



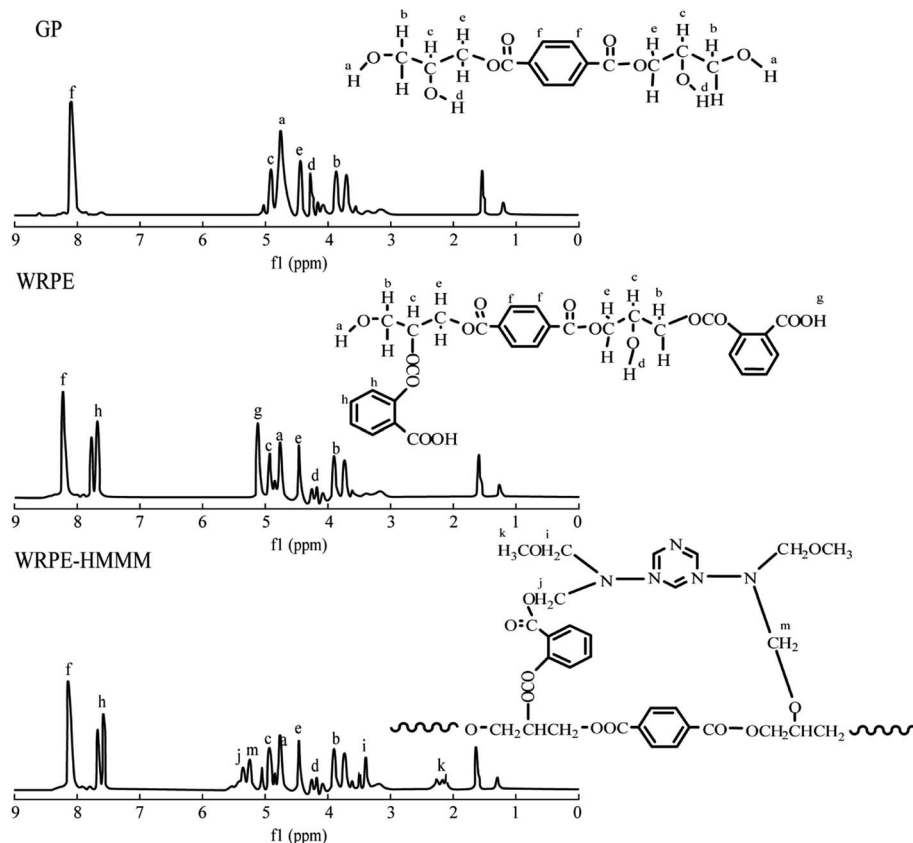


Fig. 2  $^1\text{H}$  NMR spectra of GP, WRPE, and WRPE-HMMM.

groups and protons of the aromatic ring of PET, respectively. In the WRPE spectrum, 5.11–5.19 ppm (peak *g*) and 7.39–7.69 ppm (peak *h*) indicate protons of unreacted carboxyl groups and the aromatic ring of PA bonded to the secondary hydroxyl groups of GL, respectively. In the WRPE-HMMM spectrum, 3.21–3.43 ppm (peak *k*) indicates protons of unreacted methoxy groups of HMMM, and 5.12–5.49 ppm (peak *m, j*) indicates protons of the methylene group between N and O through the curing reaction of WRPE with HMMM. The analysis shows that the reaction of GP with PA is mainly an esterification reaction, and a small amount of a polyesterification reaction of some PA with GP is performed simultaneously.

### 3.5. Characterization of the films

**3.5.1. Physicochemical properties.** Physicochemical properties of the films are shown in Table 3. Adhesion, impact strength, and flexibility of the films are important physical properties for insulation varnish. As shown in Table 3, adhesion and impact strength of the films are satisfactory. It is observed that the higher the PA content, the lower the flexibility of the film due to increase of the crosslinking density of the film. Moreover, one of the most important chemical properties of the water-based varnish is water resistance. Water resistance is generally determined by water absorption

Table 3 Physicochemical properties of the films

Sample	Adhesion (%)	Impact strength (N m)	Flexibility diameter (in)	Water absorption (%)
WRPE21	100	50	1/8	0.7
WRPE22	100	50	1/8	1.3
WRPE23	100	50	1/6	1.7
WRPE24	100	50	1/6	2.1
WRPE25	100	50	1/6	2.6
WRPE31	100	50	1/8	1.1
WRPE32	100	50	1/8	1.9
WRPE33	100	50	1/8	2.3
WRPE34	100	50	1/6	2.9
WRPE35	100	50	1/6	3.8



Table 4 Insulation properties of the films

Sample	Electrical insulation strength (kV mm <sup>-1</sup> )		Volume resistivity (Ω cm)	
	Air, 25 °C	Immersion in water for 24 h	Air, 25 °C	Immersion in water for 24 h
	WRPE21	68.7	32.3	$3.2 \times 10^{15}$
WRPE22	75.3	36.5	$6.3 \times 10^{15}$	$8.4 \times 10^{14}$
WRPE23	81.6	40.6	$1.0 \times 10^{16}$	$3.2 \times 10^{15}$
WRPE24	76.2	38.4	$8.2 \times 10^{15}$	$7.8 \times 10^{14}$
WRPE25	69.4	35.1	$7.6 \times 10^{15}$	$2.2 \times 10^{13}$
WRPE31	51.5	25.3	$5.2 \times 10^{14}$	$7.6 \times 10^{13}$
WRPE32	63.2	29.4	$9.3 \times 10^{14}$	$2.8 \times 10^{14}$
WRPE33	75.8	34.9	$5.6 \times 10^{15}$	$9.2 \times 10^{14}$
WRPE34	70.4	31.9	$3.2 \times 10^{15}$	$8.1 \times 10^{13}$
WRPE35	62.6	29.3	$1.6 \times 10^{15}$	$8.4 \times 10^{12}$

measurements. The water absorption of the films increased with increasing PA content at the same PET/GL molar ratio. This is due to higher PA content yielding higher hydrophilic group content in the polymer chain. Further, at the same PA content, the water absorption of the WRPE3 group was larger than that of the WRPE2 group. This is attributed to the fact that the average molecular weight of GP decreased with decreasing PET/GL molar ratio from 1.3 to 1.0.

**3.5.2. Insulation properties of the films.** Electrical insulation strength and volume resistivity of the film are crucial factors in the evaluation of the properties of the insulation varnish. The electrical insulation strength and volume resistivity of the films are shown in Table 4. As mentioned above, due to the average molecular weight of the WRPE2 group being larger than that of WRPE3 group at the same PA content, the electrical insulation strength and volume resistivity of the WRPE2 group are higher than those of the WRPE3 group. As the PA content increased, the electrical insulation strength and volume resistivity of the films increased at first and decreased after 10 wt%. The reason for this is that the number of aromatic rings in the polymeric structure increased with increasing PA content. However, as the carboxyl group is polar, the conductivity of the films increased with the incorporation of carboxyl groups, causing a decrease in electrical insulation strength and volume resistivity of the films. Also, the electrical insulation strength and volume resistivity of the films with different PA contents in air at 25 °C and after immersion in water for 24 h were measured. The electrical insulation strength and volume resistivity of the films in air at each given PA content are higher than those after immersion in water for 24 h. As previously mentioned, the increase in the PA content caused an increase in the water absorption. As a result, the conductivity increased and caused a decrease in the electrical insulation strength and volume resistivity of the film.

### 3.5.3. Thermal stability

**3.5.3.1. Thermogravimetric analysis.** As water absorptions of the WRPE3 group were larger than those of the WRPE2 group at the same PA content, only the thermal stability of the

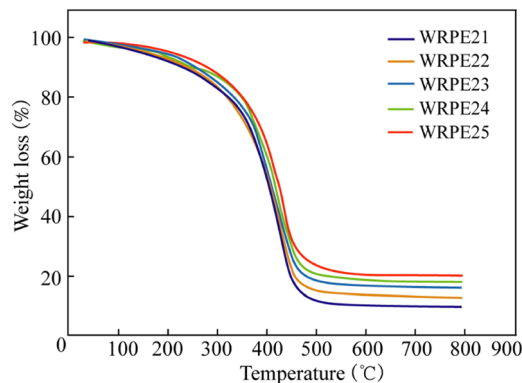


Fig. 3 Thermogravimetric analysis curves of the films: WRPE21 (5% PA content), WRPE22 (7.5% PA content), WRPE23 (10% PA content), WRPE24 (12.5% PA content), and WRPE25 (15% PA content).

WRPE2 group with different PA contents was measured in this study. Thermal stability is an important property for insulation varnish, and it is usually evaluated using TGA and DSC analysis. The TGA curves of the films with different WRPE2 groups are shown in Fig. 3. These were monitored in the temperature range of 50–800 °C with a 20 °C min<sup>-1</sup> heating rate. Fig. 3 shows that the temperatures at 50% weight loss increased from 423 to 448 °C, and those at 20% weight loss from 323 to 359 °C, with increasing PA content from 5 to 15 wt%, respectively. This aligns with the theoretical results that show that the bridge density and aromatic ring content in the polymer chain increases with increasing PA content.

**3.5.3.2. DSC analysis.** To investigate the effect of PA content on thermal stability, DSC was used to study the glass transition temperature ( $T_g$ ) of the films, and the results are shown in Fig. 4. The films with contents of PA of 5, 7.5, 10, 12.5, and 15 wt% showed  $T_g$  of approximately 145.8, 151.3, 160.2, 172.6, and 185.5 °C, respectively. An endothermic peak exists near the glass transition in each curve because of enthalpy relaxation, which occurred in the region of  $T_g$  during the heating of glass

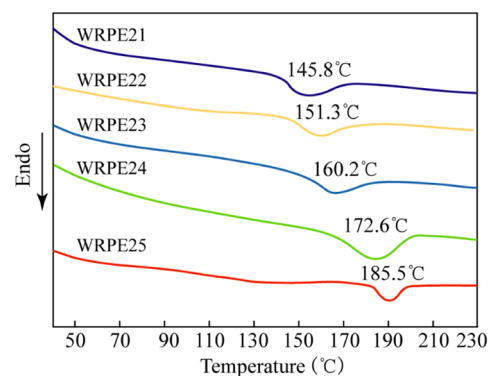


Fig. 4 DSC curves of the films: WRPE21 (5% PA content), WRPE22 (7.5% PA content), WRPE23 (10% PA content), WRPE24 (12.5% PA content), and WRPE25 (15% PA content).



materials. The DSC curves show that the  $T_g$  values of the films increased with increasing PA content. This indicates that incorporating PA had an aromatic group effect on the glass transition of the polymer. As the content of the aromatic ring in the polymer chain increased with increasing PA content, the rigidity of the polymer chain improved, and this limited the movement of the polymer segments and yielded an increase in  $T_g$ .

## 4. Conclusion

Herein, WRPE for insulation varnish was prepared from PET, GL, and PA *via* glycolysis and condensation. WRPE was dissolved in phenol, neutralized with ammonia solution, diluted in water, and cured with HMMM. The weight ratios of phenol:water (based on the total solvent) and WRPE:HMMM (based on the dry mass) were 40:60 and 70:30, respectively, and the curing temperature and time were 140 °C and 2 h, respectively. The structures of GP, WRPE, and WRPE-HMMM were investigated using FTIR and  $^1\text{H}$  NMR spectroscopy. The physical properties, such as adhesion, impact strength, and flexibility, remained unchanged, but water absorption of the film changed considerably according to PA content. As the water-dispersible stability of the WRPE1 group (PET/GL = 1.6) was low and the water absorption of the WRPE3 group (PET/GL = 1.0) was high, these groups should not be used in insulation varnish. The TGA and DSC results show that the higher the PA content, the higher the heat resistance and glass transition temperature, due to the increasing content of the aromatic ring in the polymer chain. However, when the PA content was increased, the electric insulation strength and volume resistivity of the films increased at first and then decreased above 10 wt%. WRPE23 with a PA content of 10 wt% has an excellent heat resistance grade (F grade), electrical insulation strength (81.6 kV mm<sup>-1</sup>), and volume resistivity (1.0 × 10<sup>16</sup> Ω cm in air at 25 °C and 3.2 × 10<sup>15</sup> Ω cm after immersion in water for 24 h). WRPE insulation varnish may be used for covering coils and impregnating electric motors.

## Abbreviations

WRPE	Water-reducible polyester resin
PET	Polyethylene terephthalate
GL	Glycerol
PA	Phthalic anhydride
GP	Glycolytic products
HMMM	Hexamethoxymethyl melamine resin

## Conflicts of interest

There are no conflicts to declare.

## Acknowledgements

This work is supported by National Committee of Science and Technology in DPR Korea.

## References

- 1 P. K. Maiti, Development of a silicone modified unsaturated polyester varnish for rated electrical insulation application, *IEEE Trans. Dielectr. Electr. Insul.*, 2005, **12**, 455–468.
- 2 Y. Xia, Polyester-imide solventless impregnating resin and its nano-silica modified varnishes with excellent corona resistance and thermal stability, *IEEE Trans. Dielectr. Electr. Insul.*, 2015, **22**, 372–379.
- 3 U. Jejurkar, Synthesis and characterization of novel water-soluble polyesters for electrical insulation, *J. Appl. Polym. Sci.*, 2006, **104**, 3309–3316.
- 4 Q. Ge, Synthesis, Characterization, and Properties of Acrylate-Modified Tung-Oil Waterborne Insulation Varnish, *J. Appl. Polym. Sci.*, 2014, 4610–4616.
- 5 M. R. Patel, J. V. Patel and V. K. Sinha, Glycolized PET waste and castor oil-based polyols for two-pack coating systems, *Polym. Int.*, 2006, **55**, 1315–1322.
- 6 C. Kawamura, Coating resins synthesized from recycled PET, *Prog. Org. Coat.*, 2002, **45**, 185–191.
- 7 V. Jamdar, M. Kathalewar and A. Sabnis, Glycolytic depolymerization of PET waste using MP-diol and utilization of recycled product for UV-curable wood coating, *J. Coat. Technol. Res.*, 2018, **15**, 259–270.
- 8 V. Jamdar, M. Kathalewar and R. N. Jagtap, Effect of  $\gamma$ -irradiation on glycolysis of PET waste and preparation of ecofriendly coatings using bio-based and recycled materials, *Polym. Eng. Sci.*, 2015, **55**, 2653–2660.
- 9 J. Dullius, C. Ruecker and V. Oliveira, Chemical recycling of post-consumer PET: Alkyd resins synthesis, *Prog. Org. Coat.*, 2006, **57**, 123–127.
- 10 A. Torlakoğlu and G. Güçlü, Alkyd-amino resins based on waste PET for coating applications, *Waste Manage.*, 2009, **29**, 350–354.
- 11 G. Güçlü and M. Orbay, Alkyd resins synthesized from postconsumer PET bottles, *Prog. Org. Coat.*, 2009, **65**, 362–365.
- 12 G. Güçlü, Alkyd resins based on waste PET for water-reducible coating applications, *Polym. Bull.*, 2010, **64**, 739–748.
- 13 E. U. Ikhuoria and A. I. Aigbodion, Determination of solution viscosity characteristics of rubber seed oil based alkyds resins, *J. Appl. Polym. Sci.*, 2006, **101**, 3073–3075.
- 14 K. Ertas, Alkyd resins synthesized from glycolysis products of waste PET, *Polym.-Plast. Technol. Eng.*, 2005, **44**, 783–794.
- 15 M. Ghaemy, Unsaturated polyester from glycolized PET recycled from post-consumer soft-drink bottles, Iran, *Polym. J.*, 2002, **11**, 77–83.
- 16 S. Chaeichian, Synthesis of unsaturated polyester resins from PET Wastes: Effect of a novel co-catalytic system on glycolysis and polyesterification reactions, *Des. Monomers Polym.*, 2008, **11**, 187–199.
- 17 Y. Öztürk and G. Güçlü, Unsaturated polyester resins obtained from glycolysis products of waste PET, *Polym.-Plast. Technol. Eng.*, 2010, **43**, 1539–1552.





- 18 A. M. Atta, New epoxy resins based on recycled poly (ethylene terephthalate) as organic coatings, *Prog. Org. Coat.*, 2007, **58**, 13–22.
- 19 K. Bal and K. Can, Epoxy-based paints from glycolysis products of postconsumer PET bottles: Synthesis, wet paint properties and film properties, *J. Coat. Technol. Res.*, 2017, **14**, 747–753.
- 20 A. More, Epoxy-based anticorrosive coating developed with modified poly(o-anisidine) and depolymerized product of PET waste, Iran, *Polym. J.*, 2018, **27**, 345–356.
- 21 J. Thomas, Importance and application of polyethylene terephthalate wastes in the coating industry: A review, *Int. adv. res. j. sci. eng. technol.*, 2018, **5**, 5328–5332.
- 22 E. Bulak and I. Acar, The use of aminolysis, amino-glycolysis, and simultaneous aminolysis–hydrolysis products of waste PET for production of paint binder, *Polym. Eng. Sci.*, 2014, **54**, 2272–2281.
- 23 F. Chardon, M. Denis and C. Negrell, Hybrid alkyds, the glowing route to reach cutting-edge properties?, *Prog. Org. Coat.*, 2021, **151**, 106025.
- 24 G. Colomines, J. Robin and G. Tersac, Study of the glycolysis of PET by oligoesters, *Polymer*, 2005, **46**, 3230–3247.
- 25 F. Pardal, Comparative reactivity of glycols in PET glycolysis, *Polym. Degrad. Stab.*, 2006, **91**, 2567–2578.
- 26 S. M. Cakić, Glycolyzed poly(ethylene terephthalate) waste and castor oil-based polyols for waterborne polyurethane adhesives containing hexamethoxymethyl melamine, *Prog. Org. Coat.*, 2015, **78**, 357–368.
- 27 A. Torlakoğlu, Alkyd–amino resins based on waste PET for coating applications, *Waste Manage.*, 2009, **29**, 350–354.
- 28 M. V. Gallegos and W. G. Reimers, *et. al.*, Theoretical analysis of polyethylene terephthalate (PET) adsorption on Co and Mn-doped ZnO(000-1), *Mol. Catal.*, 2022, **531**, 112688.
- 29 J. Wang, S. Zhang and Y. Han, *et. al.*, UiO66(Zr/Ti) for catalytic PET poly condensation, *Mol. Catal.*, 2022, **532**, 112741.

